ORIGINAL ARTICLE

Veterinary Research Forum. 2024; 15 (9): 487 - 498
doi: 10.30466/vrf.2024.2020333.4136
Journal Homepage: vrf.iranjournals.ir

Veterinary Research Forum

Improvement of osteogenesis and antibacterial properties of a bioactive glass/gelatin-based scaffold using zoledronic acid and CM11 peptide

Soheil Vazifehdoust[1], Ali Shalizar-Jalali[2]*, Mohammad Reza Nourani[3], Mehrdad Moosazadeh Moghaddam[3], Mohsen Yazdanian[4]

[1] PhD Candidate, Department of Basic Sciences, Faculty of Veterinary Medicine, Urmia University, Urmia, Iran; [2] Department of Basic Sciences, Faculty of Veterinary Medicine, Urmia University, Urmia, Iran; [3] Tissue Engineering and Regenerative Medicine Research Center, Baqiyatallah University of Medical Sciences, Tehran, Iran; [4] Research Center for Prevention of Oral and Dental Diseases, Baqiyatallah University of Medical Sciences, Tehran, Iran.

Article Info

Article history:

Received: 13 January 2024
Accepted: 07 April 2024
Available online: 15 September 2024

Keywords:

Bioactive glass
CM11 peptide
Mesenchymal stem cells
Osteogenesis
Zoledronic acid

Abstract

This study aimed to investigate the effects of zoledronic acid (ZA) and antibacterial CM11 peptide on the osteoinduction and antibacterial properties of bioactive glass (BG). The bioactive glass/gelatin (BG/Gel) composite was synthesized using the sol-gel method. The 2-x minimum inhibitory concentration of the peptide and 4.00 mg mL^{-1} of ZA were added to the BG/Gel during fabrication. The BG/Gel composite morphological and structural characteristics and antibacterial activities were analyzed using Fourier transform infra-red spectroscopy, scanning electron microscopy and disk diffusion test, respectively. The release of the peptide and ZA from BG/Gel was measured using ultra-violet spectroscopy. After 14 days, the effects of the peptide/ZA-containing BG/Gel (PZ-BG/Gel) on the growth and differentiation of mesenchymal stem cells were evaluated using 3-[4,5-dimethylthiazol-2-yl]-2,5 diphenyl tetrazolium bromide, calcium and alkaline phosphatase assays, immunocytochemical staining for osteocalcin (OCN) and real-time polymerase chain reaction for *OCN*, *type I collagen*, *bone morphogenetic protein 2* and *Runt-related transcription factor-2* genes. The disk diffusion test showed the anti-microbial activity of the scaffold against multi-drug-resistant isolates of *Pseudomonas aeruginosa* and *Staphylococcus aureus*. Analyses showed a significantly higher level of stem cells differentiation into the osteogenic cells in PZ-BG/Gel scaffold compared to BG/Gel scaffold alone. Accordingly, osteoblast markers were significantly increased in comparison with the control. In conclusion, the osteoinduction and antibacterial properties of BG-based scaffold can be improved using ZA and CM11.

Introduction

The Large bone defects or injuries caused by traffic accidents, old age, non-union fractures, bone tumor resection, etc., are serious problems in orthopedics, endangering people's lives.[1] Although bones have a certain healing and/or regeneration capacity, this ability is not effective for large segmental bone defects.[2] Autologous bone grafting is still considered the gold standard for repairing bone defects, but this method has disadvantages such as secondary injuries, high complications at the donor site, and limitation of specific shape. These weaknesses limit its widespread use in clinical setting.[3] On the other hand, bone allografts are alternatives to autografts, but they are expensive and carry potential risks such as adverse host immune response and disease transmission.[4] These limitations highlight the need for new approaches that can effectively promote bone regeneration.[5]

Among the new methods that have received much attention in recent years is the use of tissue engineering to repair bone injuries and promote bone regeneration. With the rapid development of tissue engineering technology, bone tissue engineering has become a promising approach for repairing bone defects.[6] Scaffolds play an important role in bone tissue engineering; through mimicking the structure and function of natural bone extra-cellular matrix (ECM). They provide a three-dimensional environment to promote adhesion, proliferation and differentiation, and possess sufficient physical properties for bone generation.[7] An ideal scaffold should be biocompatible, biodegradable, bioactive, osteoinductive and osteoconductive. In addition, bone scaffolds with biomolecules and additives such as drugs, growth factors,

***Correspondence:**

Ali Shalizar-Jalali. DVM, PhD
Department of Basic Sciences, Faculty of Veterinary Medicine, Urmia University, Urmia, Iran
E-mail: a.shalizar@urmia.ac.ir

and stem cells, can act more effectively for bone regeneration.[8] For a tissue like bone, the mechanical properties of the scaffold are crucial and the scaffold must have a high mechanical strength.[9]

According to several reports, scaffolds made from inorganic materials such as calcium phosphate-based bioceramics and bioactive glass (BG) can provide higher mechanical strength than other materials such as polymer-based scaffolds.[10] Since the discovery of 45S5 BGs by Hench, they have been considered one of the most suitable scaffold materials for bone repair.[11] It has been shown that after implantation, an amorphous calcium phosphate or crystalline hydroxyapatite phase, minerals naturally found in bone that contribute to its strength and rigidity, form on the glass surface through specific reactions, creating a strong bond with the surrounding bone tissue.[12] Former studies have also shown that BGs release ions activating the osteogenic genes expression and stimulate angio-genesis. One advantage of glasses is the ability to easily control their chemical composition and regulate degradation rates, making them attractive as scaffolding materials for bone repair.[13] The structure and chemistry of glasses can be adjusted over a wide range by changing the compounds used. The BG scaffolds are also characterized by their porous nature, numerous small voids or gaps present within the structure.[14] These pores facilitate cellular migration into the scaffold, creating a conduit for nutrient transportation, and promoting the formation of the new blood vessels through the angiogenesis process.[15] Facilitating the penetration of cells, nutrients and blood vessels into the scaffold play a crucial role in fostering the bone tissue regeneration.[16]

As mentioned, adding small biomolecules can increase the functional potential of the scaffold by regulating cellular, tissue and therapeutic functions.[17] Bisphos-phonates (BPs), pyrophosphate analogues, are small synthetic biomolecules used as drugs to stimulate the growth and differentiation of osteoblasts. This stimulation leads to bone formation and prevents bone resorption by inhibiting osteoclasts and increasing bone induction.[18] The BPs have a strong tendency to accumulate on bone surfaces which can lead to systemic side effects. However, their local delivery can effectively reduce systemic side effects and dosage. The use of BPs is considered a practical method to enhance the integration of scaffolds with surrounding bone tissue by promoting bone growth.[19]

Zoledronic acid (ZA) as a member of this group, similar to other BPs, has been shown to have the ability to enhance the proliferation and mineralization of osteoblasts.[20] Osteoblasts are specialized cells responsible for the new bone tissue formation and can be differentiated from mesenchymal stem cells (MSCs).[21] Zoledronic acid can regulate the expression of specific genes involved in osteoblast differentiation. These genes are molecular signals that guide MSCs to develop into mature osteoblasts. By influencing the expression of these genes, ZA promotes the efficient differentiation of MSCs into osteoblasts.[22]

In grafting, the risk of bacterial infections at the surgical site or on the scaffold is very high. Therefore, it is crucial to obtain scaffolds with integrated antibacterial and osteogenic functions for treating bone implant-associated infections and promoting bone repair. To address infection problems, scaffolds with various antibacterial strategies have been developed for tissue repair and regeneration. Currently, the prevalence of resistant bacterial strains is widespread, with many infections caused by multi-drug-resistant (MDR) strains that are resistant to conventional antibiotics.[23] In recent years, there has been a focus on antibacterial peptides as an alternative. These peptides are part of the innate immune system in both vertebrates and invertebrates. They are typically cationic and effective against a broad spectrum of Gram-positive and Gram-negative bacteria.[24] One such peptide is the cecropin-melittin chimeric peptide (CM11), a synthetic cationic antibacterial peptide that has demonstrated potent activities against a wide range of bacteria. This peptide is composed of 11 amino acids and has a unique amphipathic structure allowing it to interact with bacterial membranes.[25]

In line with that, this study aimed to investigate the potential of a BG scaffold containing ZA and CM11 in promoting the differentiation of human MSCs (hMSCs) into osteogenic cells as well as its antibacterial activity against MDR isolates of *Pseudomonas aeruginosa* and *Staphylococcus aureus*.

Materials and Methods

Materials. The hMSCs were provided by the Stem Cells Technology Research Center in Tehran, Iran. Ethanol, dimethyl sulfoxide (DMSO), 0.10 M nitric acid (HNO3), triethyl phosphate (TEP; C6H15O4P), calcium nitrate (Ca(NO3)24H2O), magnesium nitrate (Mg(NO3)26H2O) and tetraethylorthosilicate (TEOS; C8H20O4Si) were purchased from Merck Company (Darmstadt, Germany). The 25.00 % (w/v) glutaraldehyde (C5H8O2) solution and 10.00% w/v gelatin (Gel; microbiology grade, No.: 107040) were also purchased from Merck Company. The following agents were purchased from Sigma Company (St. Louis, USA): Chloroform, di-methyl aldehyde, penicillin/ streptomycin (Pen-Strep), trypsin-ethylenediaminetetra-acetic acid, paraformaldehyde and 3-[4,5-dimethylthiazol-2-yl]-2,5 diphenyl tetrazolium bromide (MTT) test kit. Fetal bovine serum (FBS), phosphate-buffered saline (PBS) and Dulbecco's modified Eagle medium (DMEM; high glucose) were purchased from Gibco Company (Grand Island, USA). For the evaluation of calcium content and alkaline phosphatase (ALP), two kits from Pars Azmoon (Tehran, Iran) were utilized.

Synthesis of BG. The sol-gel method was used to prepare 20.00 - 50.00 nm BG powder. At first, 13.31 mL of TEOS was added to 30.00 mL of 0.10 M nitric acid, a catalyst for hydrolysis. The mixture was then allowed to react for 30 min, so the acidic hydrolysis of TEOS proceeded to near completion. The following components were added in sequence, allowing 45 min for each component to react completely: 0.91 mL TEP, 6.14 g of calcium nitrate and 1.28 g of magnesium nitrate. After the final addition, mixing continued for 1 hr to ensure the hydrolysis reaction was complete. Once the gel had formed, it was dried in an oven and heated to 120 ˚C to remove all water. Subsequently, the powder was milled for 10 hr in a planetary mill (SVD15IG5-1; LG Co., Eschborn, Germany). The dry powder was heated to 700 ˚C to eliminate nitrates. Finally, the BG powder was prepared by the ball milling for 30 min.[26]

Fabrication of BG/Gel composition. To produce a BG/Gel composite, a homogeneous aqueous solution of gelatin (10.00% w/v) was prepared. Synthesized BG powder was added to the Gel solution to obtain a Gel (70)/BG (30) weight percent composition. After homogenization through stirring, the mixture was cast into plastic Petri dishes and frozen at –20.00 ˚C for 3 hr. To produce porous structures, the samples were transferred to a freeze-dryer (Christ Beta 2-8 LD Plus; Martin Christ Gefriertrocknungsanlagen GmbH, Osterode am Harz, Germany) at – 57.00 ˚C and 0.05 mbar for 24 hr of a three-dimensional porous structure through sublimation, forming a Gel network matrix. After freeze-drying, the composite layers were cut into predetermined sizes (scaffolds with 5.00 mm diameters).[26]

Preparation of BG/Gel composite containing CM11peptide and ZA. The *P. aeruginosa* and *S. aureus* are bacteria that cause hospital infections during surgery. In this study, according to the previous reports,[27] MDR strains of these bacteria were selected; for which the minimum inhibitory concentration (MIC) of the peptide was 8.00 µg mL^{-1}. Accordingly, to produce BG/Gel composite with antibacterial property, CM11 (Synpeptide, Shanghai, China) at 2X MIC concentration (16.00 µg mL^{-1}) was added to the BG and Gel solution during the BG/Gel composite production process. To improve osteoinduction of BG/Gel, similar to the previous study,[28] 4.00 mg mL^{-1} concentration of ZA (Sigma) was added to the BG/Gel solution along with the peptide. Then, the cross-linking of scaffolds was done in a sealed desiccator in the presence of glutaraldehyde (8.00 mL) at 37.00 ˚C for 4 hr. Afterwards, the prepared scaffolds were washed with 1.00% (w/v) of glycine solution to remove the unreacted glutaraldehyde. The fabricated scaffolds were categorized as follows: BG/Gel scaffold, BG/Gel scaffold containing CM11 peptide, BG/Gel scaffold containing ZA, and BG/Gel scaffold containing peptide and ZA (PZ-BG/Gel).

Fourier transform infra-red spectroscopy (FTIR). The FTIR analysis was conducted to identify the functional groups of the BG/Gel. For this purpose, the samples were mixed with 300 mg potassium bromide and pelletized under vacuum. The resulting pellets were subsequently analyzed in the 400 - 4,000 cm^{-1} range (ABB Bomem MB 100 Spectrometer; ABB Bomem Co., Québec, Canada).[26]

Scanning electron microscopy (SEM). Scanning electron microscopy was used to evaluate the micro-structure and morphology of the BG/Gel composite. Dry scaffold was sputter-coated with a thin layer of gold (EMITECH K450X, Quorum Technologies Ltd., Lewes, UK) and then, analyzed by a scanning electron microscope (XL30; Philips, Eindhoven, The Netherlands) operating at an accelerating voltage of 15.00 kV.

Cytotoxicity evaluation of the BG/Gel composite using MTT Assay. The cytotoxic effects of the composites (BG/Gel and PZ-BG/Gel) were evaluated using the MTT assay. The composite scaffolds were sterilized using ultraviolet (UV) irradiation for 20 min on each side, then placed inside a 96-well culture plate and washed with a sterile PBS solution. After that, the hMSCs were seeded onto the scaffolds at a density of 1.70×10^4 cells mL^{-1} by pipetting the cell suspension on the scaffolds. After one hr, DMEM (Gibco) containing 10.00% FBS (Gibco) and 100 U mL^{-1} Pen-Strep (Sigma) was added to the wells and allowed to incubate under 5.00% CO_2 at 37.00 ˚C for 24 and 48 hr. After this time, the medium was removed and 100 µL of MTT solution was added to each of the wells. Following 4 hr of incubation in the dark at 37.00 ˚C, the solution was removed and 100 µL of DMSO (Merck) was added to each well to dissolve the formazan crystals. The well without a scaffold was used as a negative control. The optical density of the solution was measured at 570 nm on an enzyme-linked immunosorbent assay plate reader (Tecan, Männedorf, Switzerland).[29]

Analysis of cell adhesion to the scaffold by SEM. Cell adhesion to the PZ-BG/Gel was analyzed by SEM. Briefly, PZ-BG/Gel was rinsed with PBS and the hMSCs were gently seeded on the scaffold by pipetting a cell suspension on the BG/Gel. After one hr, the DMEM containing 10.00% FBS was added. The cells were then cultured at 37.00 ˚C and 5.00% CO_2 for 24 hr. Then, the extent of cell attachment and growth was assessed 24 hr after cell seeding. For this purpose, seeding scaffolds were fixed by 4.00% glutaraldehyde overnight at 4.00 ˚C. After thoroughly washing with PBS, the cells were dehydrated in an ethanol-graded series (50.00 - 100%) for 10 min each and allowed to be dried on a clean bench at room temperature. The samples were subsequently characterized by SEM following gold coating.[29]

Peptide and ZA release from BG/GEL. For *in vitro* monitoring of peptide and ZA release from PZ-BG/Gel, samples were dispersed in PBS (pH: 7.40) and transferred to a dialysis bag (MWCO 12 kDa; Sigma). The dialysis bags

were immersed in a 30.00 mL of PBS and then, placed in a water bath at 37.00 ˚C and 130 rpm. At specified intervals, 1.00 mL of release medium was removed and refilled with the same volume of fresh PBS. The release amount of CM11 and ZA into the removed dialysate was determined by UV-visible spectrophotometer (Thermo Fisher Scientific, Waltham, USA) and quantified from the standard curves (λmax peptide = 278 nm and λmax ZA = 210 nm). The specified times for peptide release were at 1, 6, 12, 24, 48 and 72 hr; while, for ZA they were at 3, 6, 12 and 24 hr as well as 5, 7, 14 and 21 days.[28]

Antibacterial assay. The antibacterial activity of the scaffolds including BG/Gel (control), peptide-containing BG/Gel and PZ-BG/Gel was evaluated by agar disk diffusion method. The PZ-BG/Gel was used to determine the effect of ZA on the antibacterial activity of CM11. Briefly, 100 µL of 0.50 McFarland (1.50×10^8 CFU mL^{-1}) bacterial suspensions (*P. aeruginosa* and *S. aureus*) were cultured on Mueller-Hinton Agar plates. Disks of the samples (0.50 cm in diameter) were then placed on the plates and incubated at 37.00 ˚C for 24 hr. The zone of inhibition around the disks was measured as an indicator of the anti-microbial activity of the scaffold.[29]

Differentiation of hMCs. Before seeding the cells on BG/Gel and PZ-BG/Gel scaffolds, they were sterilized by UV irradiation for 20 min on each side. The hMCSs were seeded on scaffolds using DMEM with 10.00% FBS and 1.00% Pen-Strep, followed by incubation at humidified condition with 5.00% CO_2 at 37.00 ˚C. Also, the osteogenic agents including 50.00 µg mL^{-1} L-ascorbic acid, 10,000 µM beta-glycerophosphate and 10^{-4} µM dexamethasone were added to the medium. The medium was changed every 3 days. After 14 days, the cells were harvested to evaluate their differentiation efficacy.

Alkaline phosphatase activity assay. The ALP activity assay was performed using 200 µL of radioimmunoprecipitation lysis buffer. Total protein was extracted from hMSCs cultured on scaffolds after 14 days. For cell debris sedimentation, the lysate was centrifuged at 1,200 rpm at 4.00 ˚C for 5 min. The supernatant was then collected and ALP activity was examined with an ALP Assay Kit using a micro-plate reader at 405 nm.[30]

Calcium assay. Calcium deposition on the scaffolds was examined using alizarin red staining method. After 14 days of incubation of hMSCs on scaffolds, the fixation of cell-scaffold constructs was performed. Accordingly, samples were rinsed with PBS and then, dehydration of samples was performed through graded concentrations of ethanol (50.00, 70.00, 80.00, 96.00, and 100%) for 10 min, respectively. For staining, the alizarin red (40.00 mM) was poured on the samples and kept for 20 - 30 min. The deposited calcium appeared as a red/purple color was then observed using an inverted optical microscope (Eclipse TE2000-U; Nikon, Tokyo, Japan).[30]

Gene expression analysis using real-time polymerase chain reaction (PCR). The hMSCs differentiation and osteogenesis were analyzed through evaluation of the expression level of four genes related to osteogenesis including *osteocalcin* (*OCN*), *type I collagen* (*COL-I*), *bone morphogenetic protein 2* (*BMP-2*) and *Runt-related transcription factor-2* (*RUNX2*) using real-time PCR. For this purpose, scaffolds were placed on a 6-well plate, then the stem cells were cultured and an osteogenic medium was added. The BG/Gel scaffold was also considered as a control. To evaluate the differentiation efficacy, the cell-seeded scaffolds were harvested and dissolved in chloroform. To extract total RNA from samples, Gene-MATRIX Universal RNA Purification Kit (EURx®, Gdansk, Poland) was used. The quality and quantity of samples were determined by measuring optical density at 260 and 280. According to the manufacturer's protocol, cDNA was synthesized using PrimeScript™ RT Reagent Kit Perfect Real-Time (TaKaRa Bio Inc., Kusatsu, Japan). The SYBR green master mix (Ampliqon, Odense, Denmark) was also used to perform quantitative PCR. The following parameters were used to amplify osteogenesis-related genes with *β-actin* as a reference gene: Initial denaturation at 92.00 ˚C for 5 min; 40 cycles of denaturation (92.00 ˚C for 30 sec), annealing (58.00 ˚C for 30 sec), extension (72.00 ˚C for 30 sec), and final extension for 10 min at 72.00 ˚C. The sequences of primers are presented in Table 1 and relative gene expression was calculated using $2^{-\Delta\Delta CT}$ method.[30]

Table 1. Primer sequences used in real-time polymerase chain reaction analysis.[30,31]

Genes	Primer sequence	Amplicon size (bp)
COL-I	F: 5'- TGG AGC AAG AGG CGA GAG -3' R: 5'- CAC CAG CAT CAC CCT TAG C -3'	257
RUNX2	F: 5'- GCC TTC AAG GTG GTA GCC C -3' R: 5'- CGT TAC CCG CCA TGA CAG TA -3'	197
OCN	F: 5'- GCA AAG GTG CAG CCT TTG TG -3' R: 5'- GGC TCC CAG CCA TTG ATA CAG -3'	242
BMP-2	F: 5'- AAC AAT GGC ATG ATT AGT GG -3' R: 5'- TTG GAG GAG AAA CAA GGT G -3'	264
β-actin	F: 5'- ATG CTG CTT ACA TGT CTC GAT- 3' R: 5'- AGC AGA GAA TGG AAA GTC AAA- 3'	330

OCN: *Osteocalcin*; *COL-I*: *Type I collagen*; *BMP-2*: *Bone morphogenetic protein 2*; *RUNX2*: *Runt-related transcription factor-2*.

Immunocytochemical (ICC) staining for OCN protein. Immunocytochemistry was used to investigate the post-translational of the OCN expression in differentiated hMSCs after 14 days growing on scaffolds. Briefly, cell-cultured scaffolds were fixed with 4.00% para-formaldehyde for 20 min at room temperature. After that, scaffolds were rinsed in 1.00% bovine serum albumin for blocking and then, incubated at 4.00 ˚C for one hr. Anti-OCN (1:50; Abcam, Cambridge, USA) was used as a primary antibody, followed by fluorescein isothiocyanate-conjugated goat-anti-mouse immuno-globulin G (1:200; Sigma) as a secondary antibody. Before imaging, the supernatant was removed and 4′,6-diamidino-2-phenylindole (DAPI) was then used for staining the cell nucleus.[32]

Statistical analysis. All experiments were conducted in triplicate and the results were presented as the mean value accompanied by the standard deviation. The statistical analysis of the results was performed using the Wilcoxon rank test and ANOVA test using GraphPad Prism Software (version 9.0; GraphPad Software Inc., USA) and SPSS Software (version 22; IBM SPSS Statistics, USA). A significance level of $p < 0.05$ was considered for all statistical tests.

Results

FTIR analysis. The spectrum reveals the functional groups of the BG/Gel in the spectral range of 400 - 4,000 cm^{-1} recorded after synthesis of the composite (Fig. 1). The FTIR spectra showed vibration bands at 924 and 998 cm^{-1}, which are related to the symmetric and asymmetric stretching Si–O–Si bending modes. Bands positioned at 1,458 and 1,733 cm^{-1} are related to the silicate network and ascribed to the LO mode of Si–O–Si and Si–O stretching of non-bridging oxygen atoms, respectively. In addition, vibration band at 849 cm^{-1} is related to the (PO4)3. The analysis represents the FTIR spectrum of the BG/Gel exhibiting a number of new characteristic spectral bands related to the protein spectra such as N–H bending vibration at 1,260 cm^{-1} and 1,560 cm^{-1}, for the amide III and amide II, respectively, and C=O stretching vibration at 1,670 cm^{-1} for the amide I. In addition, C–H bending vibration at 2,952 cm^{-1} represents amide B and band at 3,570 cm^{-1} indicates the presence of O–H groups.

Analysis of BG/Gel by SEM. The SEM was used to observe the morphology of BG/Gel scaffold. The SEM micrograph images confirmed the porous and nano-structure of the composite (Fig. 2).

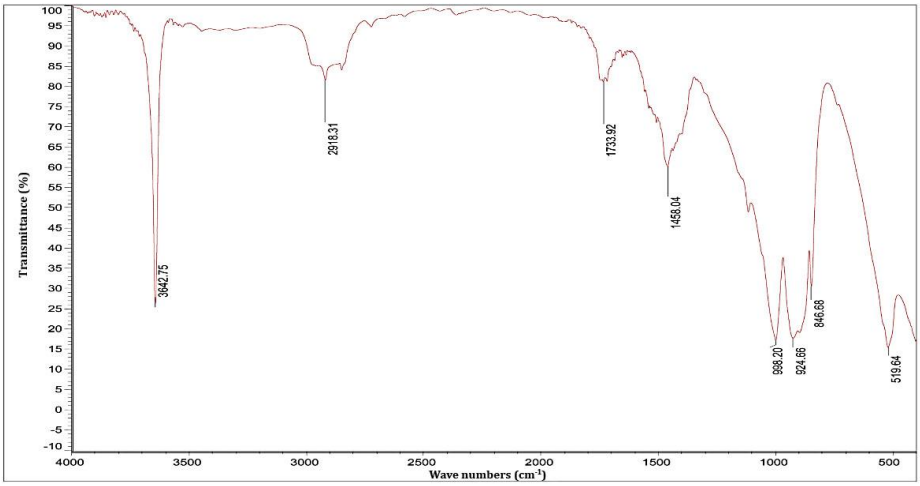

Fig. 1. The Fourier transform infrared spectroscopy spectra of the bioactive glass-gelatin composite.

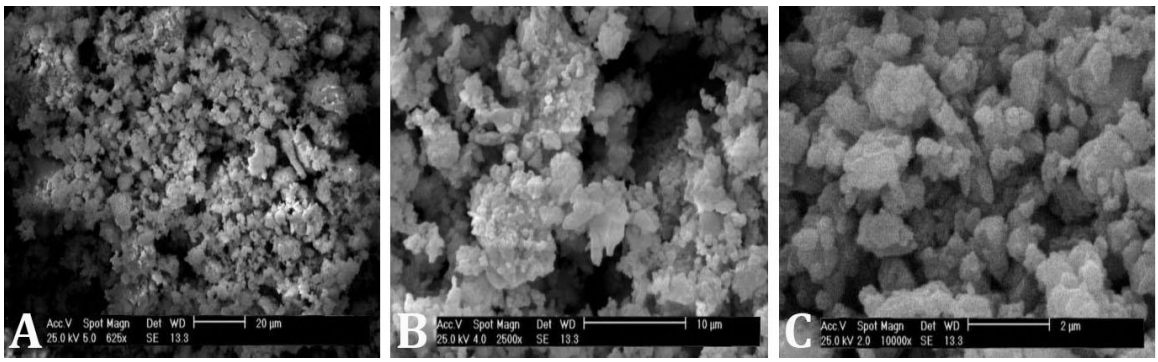

Fig. 2. Analysis of micro-structure and morphology of the bioactive glass-gelatin scaffold using scanning electron microscopy (SEM). **A-C)** The SEM micrograph images confirmed the porous and nanostructure of the composite.

Cytotoxicity and cell adhesion. In Figure 3, cell viability and cytocompatibility of the BG/Gel (control) and PZ-BG/Gel scaffolds and in Figure 4, cell adhesion to the PZ-BG/Gel scaffold are shown. The MTT assay showed that cell viability of hMSCs cultured on BG/Gel scaffold was not significantly different from the control group during 24 and 48 hr. In addition, comparison of the results after 24 and 48 hr showed significantly higher cell viability in PZ-BG/Gel scaffolds than others ($p < 0.05$; Fig. 3). These results clearly suggest that the fabricated scaffolds were non-toxic. Adhesion of cells to scaffolds is a direct indicator of cell-scaffold compatibility. As can be seen in Figure 4, the cells have proliferated well on the surface of the scaffold.

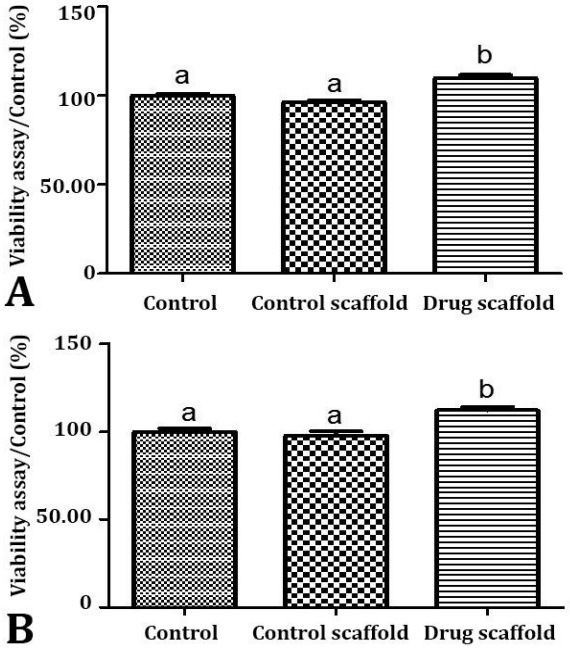

Fig. 3. Cell viability results of human adipose-derived mesenchymal stem cells cultured on tissue culture plate (Control), bioactive glass-gelatin (BG/Gel) scaffold (Control scaffold) and peptide/ zoledronic acid-containing BG/Gel scaffold (Drug scaffold). The cell viability was analyzed after **A)** 24 hr and **B)** 48 hr. [ab] Different letters indicate a significant difference.

***In vitro* release study.** Local drug delivery with controlled behavior can lead to a reduction in side effects and greater effectiveness. When evaluating the release behavior, the release of ZA began with a low burst mode and then continued through a sustained release at a low rate (Fig. 5A). The release profile was evaluated up to day 21, showing a sustained release that is highly suitable for *in vitro* osteogenic differentiation. The evaluations indicated that approximately 35.00% of the ZA was released within the 1st 24 hr, with a slower release rate thereafter. By the 5th (120 hr) and 21st days (504 hr), 50.00%, and 75.00% of the ZA were released, respectively. To evaluate the peptide release behavior from the scaffold, the scaffold containing 16.00 µg mL^{-1} of peptide was considered. As shown in Figure 5B, there was a rapid release of CM11 from the scaffold after 12 hr (about 45.00%). Following this initial release, there was a gradual increase in the amount of CM11 released from the scaffold, displaying a slow and linear trend. After 72 hr, over 80.00% of the peptide was released from the scaffold.

Antibacterial activity. According to the results obtained from the disk diffusion test, as represented in Figure 6, the BG/Gel scaffold indicated no antibacterial activity against MDR isolates of *S. aureus* and *P. aeruginosa*. However, in BG/Gel scaffolds loaded with CM11 and peptide/ZA, respectively, a lack of bacterial growth zone was observed. These results showed that the CM11 load in the scaffold led to the induction of antibacterial properties, which was not related to the presence or absence of ZA.

Calcium content. The results of calcium content assay on day 14 are represented in Figures 7 and 8. According to the results, the calcium content was significantly higher in PZ-BG/Gel scaffold than BG/Gel one. The quantitative analysis of differentiation based on calcium content showed a significant increase in stem cell differentiation into the osteoblasts in the scaffold loaded with ZA compared to the control (BG/Gel), reaching approximately 70.00%, while the scaffold alone exhibited around 50.00% differentiation (Fig. 7A; $p < 0.05$).

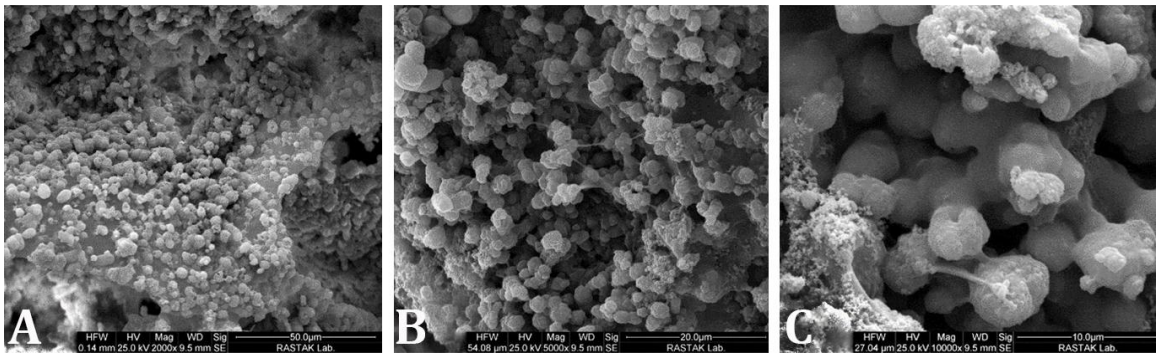

Fig. 4. Analysis of human adipose-derived mesenchymal stem cells adhesion on the drug scaffold using scanning electron microscopy. **A-C)** The cells were proliferated well on the surface of scaffold, indicating of cell-scaffold compatibility.

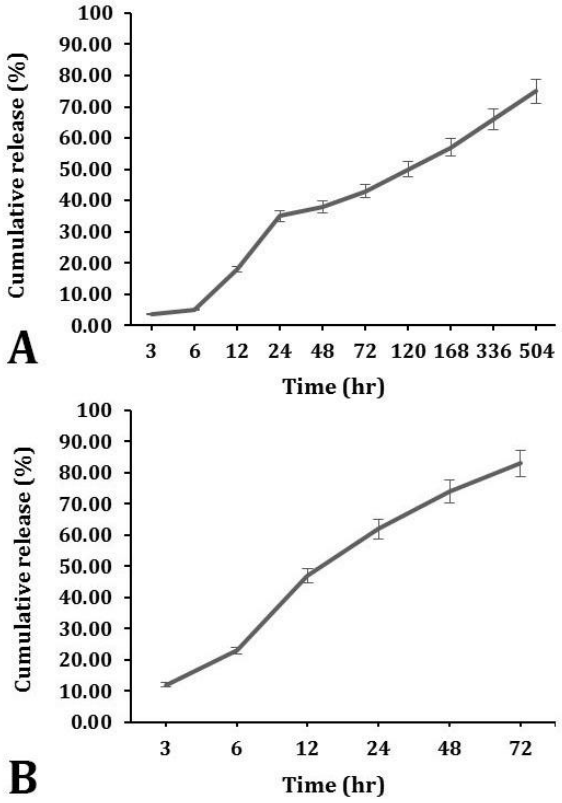

Fig. 5. The release profile of **A)** zoledronic acid (ZA) and **B)** peptide (from the peptide/ZA-containing bioactive glass-gelatin scaffold. A rapid release of the ZA at 24 hr and peptide at 12 hr is visible. An increase in the release with a linear pattern can be observed up to hr 500 and 72 for ZA and peptide, respectively, resulting in the release of ~ 80.00% of the drugs.

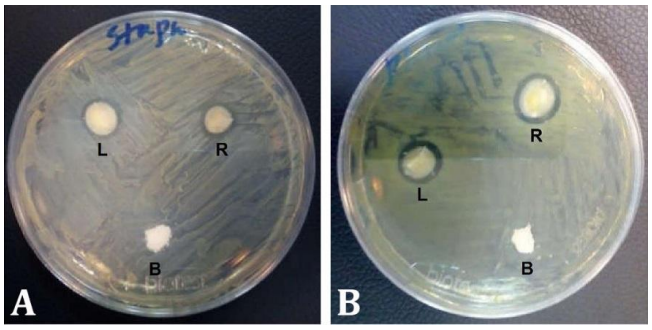

Fig. 6. Evaluation of the antibacterial activity of bioactive glass-gelatin (BG/Gel; B disk), peptide-containing BG/Gel (L disk) and peptide/zoledronic acid (ZA)-containing BG/Gel (R disk) scaffolds against **A)** *Staphylococcus aureus*, and **B)** *Pseudomonas aeruginosa* by disk diffusion test. After 24 hr, a halo around peptide-BG/Gel and peptide/ZA-BG/Gel scaffolds was detectable in Mueller-Hinton Agar plates compared to the BG/Gel as a control disk.

Alkaline phosphatase activity. The results of ALP activity in hMSCs on BG/Gel and PZ-BG/Gel scaffolds after 14 days are illustrated in Figure 7B. The level of ALP activity in the cells differentiated on the BG/Gel scaffold loaded with ZA was significantly higher than the cells differentiated on the BG/Gel scaffold without ZA ($p < 0.05$). As shown in Figure 7B, the activity level of the ALP in the test group is more than two times higher than that of the control group.

Osteogenic genes expressions. The results or real-time PCR are shown in Figure 9. The findings were in line with the results of ALP activity and calcium content. The expression level of *OCN*, *RUNX-2*, *BMP-2* and *COL-I* genes in the seeded hMSCs on the PZ-BG/Gel scaffold was significantly ($p < 0.05$) higher than the control group, demonstrating the significant impact of ZA on the differentiation of hMSCs into osteoblasts.

Immunocytochemical staining of differentiated cells. The results of the immunocytochemistry are represented in Figure 10, confirming higher expression of OCN in the hMSCs seeded on the ZA-containing BG/Gel scaffold (Fig. 10A) than BG/Gel scaffold (Fig. 10B). The DAPI staining was also carried out, showing the proliferation of seeded cells on both scaffolds. Based on the ICC analysis, it can be concluded that loading of ZA in BG/Gel scaffold has promoted osteogenic differentiation. The quantitative analyses of ICC (Fig. 11) indicated that the expression of OCN in differentiated cells on PZ-BG/Gel scaffold (approximately 60.00%) was significantly higher than control group (approximately 40.00%; $p < 0.05$).

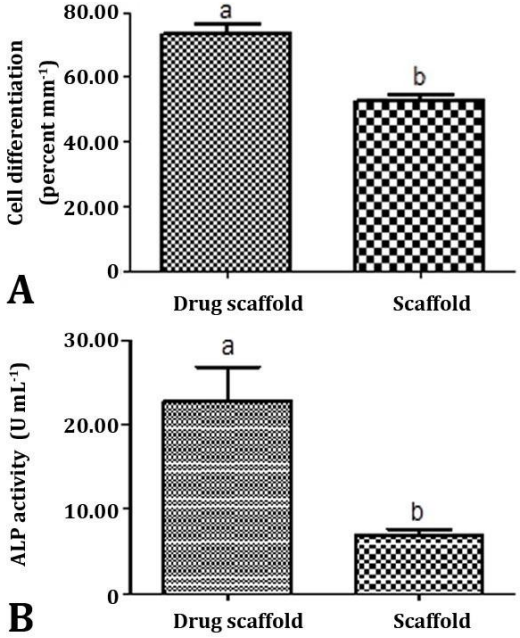

Fig. 7. Human adipose-derived mesenchymal stem cells differentiation analysis. **A)** This graph shows the rate (%) of cell differentiation based on calcium staining. The level of differentiation in the peptide/ zoledronic acid (ZA)-containing bioactive glass-gelatin (BG/Gel; Drug scaffold) scaffold is significantly higher than control one (Scaffold). **B)** Alkaline phosphatase (ALP) activity of BG/Gel (Scaffold) and peptide/ZA-containing BG/Gel (Drug scaffold) scaffolds on day 14 during osteogenic differentiation. [ab] Different letters indicate a significant difference ($p < 0.05$).

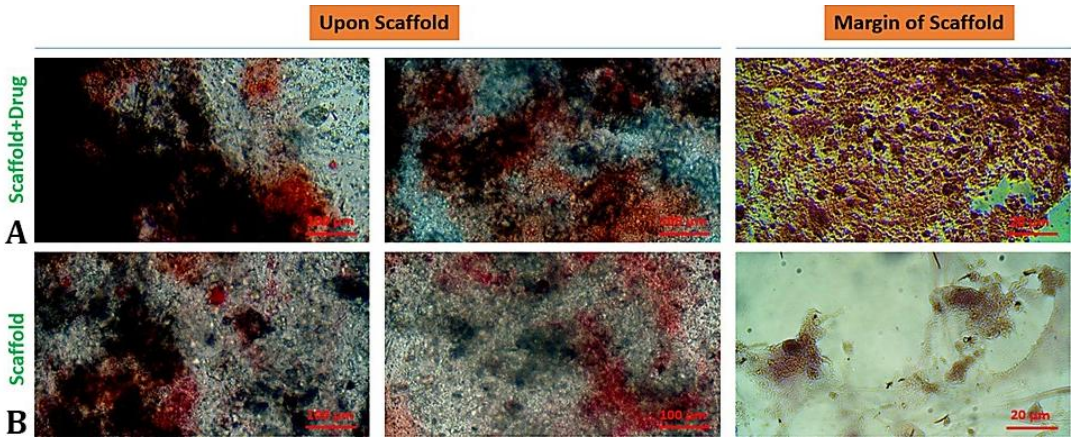

Fig. 8. Human adipose-derived mesenchymal stem cells (hMSCs) differentiation analysis. Alizarin red staining of seeded hMSCs on **A)** Peptide/zoledronic acid-containing bioactive glass-gelatin (BG/Gel), and **B)** BG/Gel scaffolds on day 14.

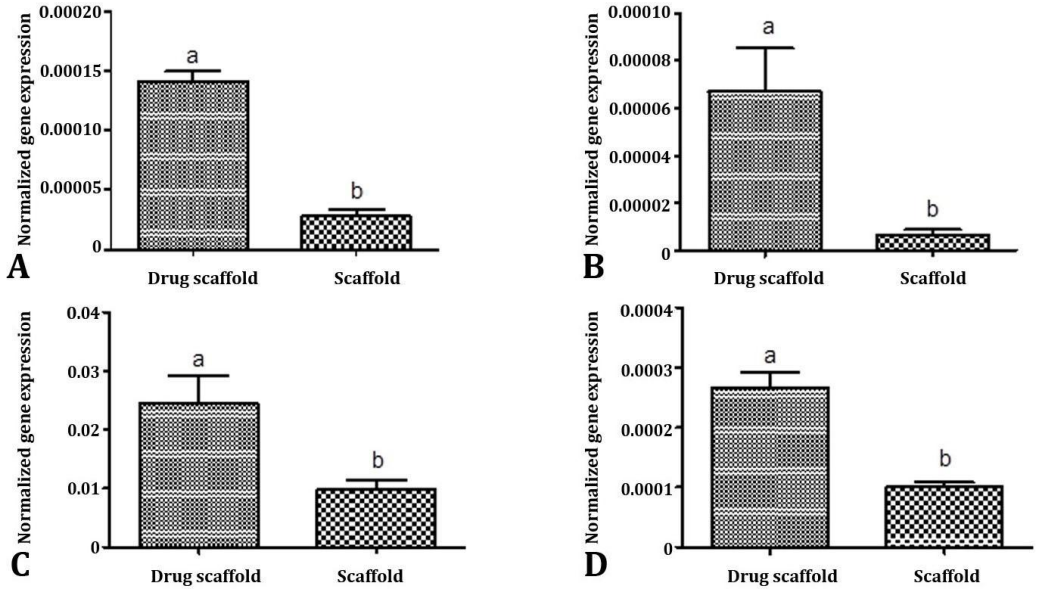

Fig. 9. The expression level of osteogenic genes in seeded human adipose-derived mesenchymal stem cells on the peptide/zoledronic acid-containing bioactive glass-gelatin (BG/Gel; Drug scaffold) and BG/Gel scaffolds on day 14. Significant higher expression of **A)** *Osteocalcin*, **B)** *Runt-related transcription factor-2*, **C)** *Bone morphogenetic protein 2,* and **D)** *Collagen-1* genes was observed in cells seeded on Drug scaffold compared to BG/Gel (Scaffold; $p < 0.05$). [ab] Different letters indicate a significant difference ($p < 0.05$).

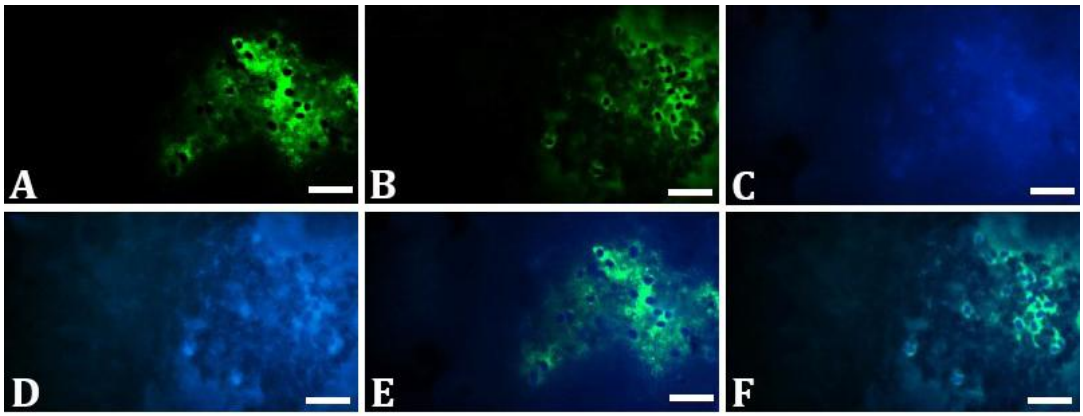

Fig. 10. Osteocalcin-based immunocytochemistry (green; **A** and **B**) and 4′,6-diamidino-2-phenylindole (DAPI; blue [**C** and **D**]) staining of the seeded human adipose-derived mesenchymal stem cells on the peptide/zoledronic acid-containing bioactive glass-gelatin (BG/Gel; **A**, **C**, and **E**) and BG/Gel (**B**, **D**, and **F**) on day 14. **E** and **F**: Merged.

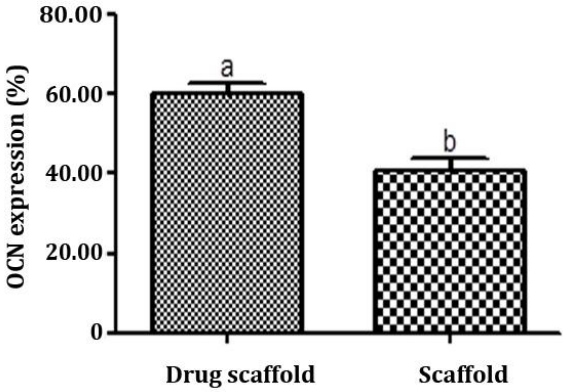

Fig. 11. Quantitative analyses of immunocytochemical staining. The graph shows the rate (%) of osteocalcin (OCN) expression in differentiated human adipose-derived mesenchymal stem cells on scaffolds. As shown, the differentiation level in the Drug scaffold group is significantly ($p < 0.05$) higher than control one. [ab] Different letters indicate a significant difference.

Discussion

Tissue engineering uses stem cells, induced components and a chemical substrate to help reconstruct whole organs or tissues.[33] For bone regeneration, various stem cell types, growth stimulants and polymers have been used.[34] In this study, a BG/Gel composite scaffold loaded with CM11 and ZA was successfully developed to enhance bone tissue regeneration. The results obtained demonstrated the scaffold's potential to promote osteogenic differentiation of hMSCs and inhibit bacterial growth, making it a promising candidate for bone tissue engineering applications.

The FTIR analysis provided valuable insights into the chemical composition of the BG scaffold. The presence of characteristic bands corresponding to Si-O-Si bending modes and silicate network vibrations in the BG spectrum confirmed the successful fabrication of the BG component. The FTIR analysis also confirmed the successful incorporation of Gel into the BG scaffold, as evidenced by the characteristic peaks corresponding to protein spectra such as N-H bending and C=O stretching vibrations. This indicates the presence of Gel in the composite, which can enhance cell adhesion and matrix mineralization, crucial for promoting bone tissue formation.[35] Furthermore, SEM analysis revealed the highly porous and nanostructured morphology of the BG/Gel scaffold, essential for nutrient diffusion, waste removal and providing a favorable micro-environment for cell growth and differentiation. The electrospinning technique used to fabricate the scaffold allowed the formation of fibers with controllable diameters, mimicking the natural ECM's fibrous structure and enhancing cell-scaffold interactions.[36]

In this study, cytotoxicity and cell adhesion showed that BG/Gel scaffold containing the peptide and ZA was biocompatible and supported the cell proliferation. The lack of significant cytotoxic effects and well-proliferated cells on the scaffold surface confirmed its potential for bone tissue engineering.[37] One important feature of this scaffold was its antibacterial properties, which were associated with the cationic antibacterial peptide called CM11 and its controlled release. Cationic peptides, which are short and positively charged peptides with antibacterial activities against a wide range of bacteria, have been recently proposed as suitable alternatives to conventional antibiotics.[38] In several organisms, these peptides are vital components of the defense mechanism against infections. Cationic anti-microbial peptides (CAMPs) such as CM11 act against infection through modulating the immune system, controlling inflammation and disrupting bacterial cell membrane function. Former studies have shown that the electrostatic binding caused by the negative charge of the outer membrane structures of the bacterial cell, such as lipopolysaccharides, and the positive charge of cationic peptides are the main factors involving in the effect of peptides on bacterial cells. The amphipathic nature of the peptide also plays an important role; it attaches to the membrane and penetrates into the membrane structure from the hydrophobic region and causes bacterial death via creating a pore.[25,39] Accordingly, several recent studies have focused on the evaluation and production of CAMPs with significant antibacterial effects and low cytotoxicity, especially to combat resistance strains causing tissue infection.[40] Cationic CM11, a synthetic hybrid derived from cecropin and melittin peptides, has been shown to have significant antibacterial activity against several human pathogens as well as trivial cytotoxic and hemolytic effects.[25,41]

The findings of this study showed that the presence of CM11 led to the antibacterial properties induction in the BG/Gel, as evidenced by the results of disk diffusion. According to the results obtained, the peptide-containing scaffold effectively prevented the growth of antibiotic-resistant *P. aeruginosa* and *S. aureus* isolates compared to the control group, which can significantly reduce the risk of infection with these bacteria during grafting. On the other hand, continuous and stable antibiotic release is a crucial factor in infection control. In this study, as mentioned, BG/Gel scaffold exhibited a prompt release of the peptide within 12 hr (about 45.00%), followed by a gradual increase in release over time. The sustained release of CM11 from the scaffold is critical for providing long-term antibacterial protection, reducing the infections risk and ensuring successful bone regeneration.[42] In addition, the antibacterial results related to the BG/Gel scaffold containing peptide and peptide/ZA were similar, confirming that the ZA did not affect the antibacterial activity of the peptide.

Reportedly, it has been shown that ZA can effectively play a role in increasing the differentiation of stem cells into the osteogenic cells. However, since the systemic

release of ZA can lead to significant side effects, its controlled and local release should be considered in order to reduce the adverse effects effectively.[28,43] Considering that scaffolds based on BG are very effective in bone tissue engineering, and on the other hand, ZA has also been shown to be effective in stimulating cell differentiation into the osteogenic cells, the osteogenic effects of the BG/Gel containing ZA were compared to the BG/Gel alone and the release behavior of ZA from scaffold was evaluated. The release behavior of ZA started with a burst release in the first 24 hr (about 35.00%) and subsequently the release continued with a mild linear trend. After 72 hr, about 75.00% of the ZA was released, which was similar to the reported release behavior of ZA from Gel-halloysite nanotubes /ZA scaffold,[28] which has the capacity to carry and release ZA sustainably and promote osteogenesis. Similarly, in the present study, the release of ZA continued for 21 days, which can significantly affect the differentiation of stem cells into the osteogenic cells.

Therefore, loading ZA into a BG/Gel scaffold can effectively promote differentiation of hMSCs and osteogenesis, as molecular evaluations have also confirmed. Our evaluations showed a significant increase in ALP activity, calcium content and expression level of selected genes compared to the control scaffold.

The ALP is a surface protein being considered as a marker of early bone differentiation for the screening of pre-osteoblasts. Findings have shown that the expression of this protein up-regulates in the first 2 days of the differentiation process. Cells with high levels of ALP expression do not divide, but they modulate OCN synthesis to direct the differentiation of pre-osteoblasts into osteoblasts.[30,44] Our results after 14 days showed that the activity level of ALP in the cells seeded on the BG/Gel scaffold loaded with the ZA was significantly higher than the scaffold without the ZA, indicating a greater stimulation of the differentiation due to the ZA. Alizarin red staining was used to examine calcium deposition, serving as a late marker of osteogenesis.[45]

The amount of calcium deposition was visible as red dots in the scaffolds. On the 14th day, a comparative evaluation between the BG/Gel scaffold with ZA and the scaffold without ZA showed that the amount of calcium deposition on the ZA-BG/Gel was significantly higher, indicating elevated osteogenesis regarding to the release of ZA from the scaffold. These findings are consistent with the previous report,[28] showing that the presence of ZA can lead to an increase in ALP activity and calcium content.

Additionally, the expression of genes related to osteogenesis showed that in the cells seeded on BG/Gel containing ZA, the expression level of these genes was remarkably higher compared to the cells seeded on the scaffold without ZA. In general, during osteogenesis, pre-osteoblasts are first formed from MSCs, which are a common progenitor for bone and cartilage cells. As differentiation progresses, similar cells accumulate through a process called crowding, accompanied by an increase in the number of committed pre-osteoblasts differentiating into the osteoblasts. Next, these cells secrete a non-mineral matrix forming the osteoid. Osteoids eventually give rise to the mature osteocytes through mineralization.[46] This process is regulated by *RUNX2* through controlling the expression of key factors involved in osteogenesis such as *COL-I* and ALP.

The *COL-I* is an early marker of osteoblasts and an increase in the expression level of *COL-I* is observed during transformation of osteoprogenitors to the pre-osteoblasts. Pre-osteoblasts are cuboidal cells producing large amounts of *COL-1*. It has been shown that as these cells progress towards osteogenic commitment, the levels of ALP and osteonectin increase significantly in them.[30,46]

The evaluation of *BMP-2* expression levels also showed a significant increase in the cells cultured on the ZA-containing BG/Gel compared to the cells on the BG/Gel scaffold alone. The BMP is a member of the transforming growth factor-β superfamily, predominantly synthesized and secreted by osteoblasts. Previous studies have demonstrated that *BMP-2* facilitates the osteogenic differentiation of MSCs *via* inducing ALP activity, promoting mineralization, enhancing adherence and mediating the expression and activation of certain associated osteogenic markers.[31]

Accordingly, all findings in this study showed that the ZA effectively increased the osteogenic differentiation of MSCs. The ICC also supported the enhanced osteogenic differentiation of hMSCs cultured on ZA-containing BG/Gel scaffold. Further, higher expression of *OCN* indicates more mature osteoblasts.

Finally, the BG/Gel composite scaffold loaded with CM11 and ZA demonstrates promising potential for bone tissue engineering applications. The combination of BG and Gel with controlled peptide and ZA release offers a versatile platform for promoting osteogenesis and preventing bacterial infections. This novel scaffold presents a valuable addition to the existing repertoire of bone tissue engineering approaches, offering tailored solutions for complex bone defects and infections. Continued research and collaboration with other biomaterials and osteoinductive factors will drive the advancement of tissue engineering strategies, ultimately bringing personalized and regenerative treatments closer to the clinical reality. As with any study, there are limitations warranting consideration. While we have demonstrated the potential of the BG/Gel scaffold for bone tissue engineering *in vitro*, further investigations are needed to assess its behavior *in vivo* using animal models. Additionally, optimization of the release kinetics of CM11 and ZA is necessary to achieve the ideal balance between the antibacterial activity and osteoinductive potential.

In conclusion, our findings underscore the significant contributions of our BG/Gel scaffold, which combines bioactivity, controlled peptide and ZA release and osteoinductive properties. With continued research and refinement, this scaffold holds promise as a transformative approach in bone tissue engineering. It offers hope for improved patient outcomes and enhanced regenerative therapies. Clarification of the detailed micro-structural characteristics of this scaffold using electron paramagnetic resonance spectroscopy as well as X-ray diffraction technique is highly suggested for upcoming studies.

Acknowledgments

The authors are grateful for the supports of the Urmia University, Urmia, Iran, and Baqiyatallah University of Medical Sciences, Tehran, Iran.

Conflict of interest

There is no conflict of interest to declare.

References

1. Kaewpornsawan K, Eamsobhana P. Free non-vascularized fibular graft for treatment of large bone defect around the elbow in pediatric patients. Eur J Orthop Surg Traumatol 2017; 27(7): 895-900.
2. Oryan A, Alidadi S, Bigham-Sadegh A, et al. Effectiveness of tissue engineered based platelet gel embedded chitosan scaffold on experimentally induced critical sized segmental bone defect model in rat. Injury 2017; 48(7): 1466-1474.
3. 3. Schmidt AH. Autologous bone graft: is it still the gold standard? Injury 2021; 52(Suppl 2): S18-S22.
4. Kong CH, Steffi C, Shi Z, et al. Development of mesoporous bioactive glass nanoparticles and its use in bone tissue engineering. J Biomed Mater Res B Appl Biomater 2018; 106(8): 2878-2887.
5. Zhang LY, Bi Q, Zhao C, et al. Recent advances in biomaterials for the treatment of bone defects. Organogenesis 2020; 16(4): 113-125.
6. Vadaye Kheiry E, Fazly Bazzaz BS, Kerachian MA. Implantation of stem cells on synthetic or biological scaffolds: an overview of bone regeneration. Biotechnol Genet Eng Rev 2021; 37(2): 238-268.
7. Fattahi R, Mohebichamkhorami F, Taghipour N, et al. The effect of extracellular matrix remodeling on material-based strategies for bone regeneration: review article. Tissue Cell 2022; 76: 101748. doi: 10.1016/j.tice.2022.101748.
8. Sow WT, Wang Y, Chen L, et al. Freeze-casted keratin matrix as an organic binder to integrate hydroxy-apatite and BMP2 for enhanced cranial bone regeneration. Adv Healthc Mater 2023; 12(16): e2201886. doi: 10.1002/adhm.202201886.
9. Firouzian KF, Song Y, Lin F, et al. Fabrication of a biomimetic spinal cord tissue construct with heterogenous mechanical properties using intrascaffold cell assembly. Biotechnol Bioeng 2020; 117(10): 3094-3107.
10. Faqhiri H, Hannula M, Kellomäki M, et al. Effect of melt-derived bioactive glass particles on the properties of chitosan scaffolds. J Funct Biomater 2019; 10(3): 38. doi: 10.3390/jfb10030038.
11. Fernandes HR, Gaddam A, Rebelo A, et al. Bioactive glasses and glass-ceramics for healthcare applications in bone regeneration and tissue engineering. Materials (Basel) 2018; 11(12): 2530. doi: 10.3390/ma11122530.
12. Von Euw S, Ajili W, Chan-Chang TH, et al. Amorphous surface layer versus transient amorphous precursor phase in bone - a case study investigated by solid-state NMR spectroscopy. Acta Biomater 2017; 59: 351-360.
13. Abodunrin OD, El Mabrouk K, Bricha M. A review on borate bioactive glasses (BBG): effect of doping elements, degradation, and applications. J Mater Chem B 2023; 11(5): 955-973.
14. Nommeots-Nomm A, Labbaf S, Devlin A, et al. Highly degradable porous melt-derived bioactive glass foam scaffolds for bone regeneration. Acta Biomater 2017; 57: 449-461.
15. Diomede F, Marconi GD, Fonticoli L, et al. Functional relationship between osteogenesis and angiogenesis in tissue regeneration. Int J Mol Sci 2020; 21(9): 3242. doi: 10.3390/ijms21093242.
16. Chen J, Li Y, Liu S, et al. Freeze-casting osteochondral scaffolds: the presence of a nutrient-permeable film between the bone and cartilage defect reduces cartilage regeneration. Acta Biomater 2022; 154: 168-179.
17. Park JY, Gao G, Jang J, et al. 3D printed structures for delivery of biomolecules and cells: tissue repair and regeneration. J Mater Chem B 2016; 4: 7521-7539.
18. Endo Y, Funayama H, Yamaguchi K, et al. Basic studies on the mechanism, prevention, and treatment of osteonecrosis of the jaw induced by bisphosphonates [Japanese]. Yakugaku Zasshi 2020; 140(1): 63-79.
19. Chen Y, Wu X, Li J, et al. Bone-targeted nanoparticle drug delivery system: an emerging strategy for bone-related disease. Front Pharmacol 2022; 13: 909408. doi: 10.3389/fphar.2022.909408.
20. Scala R, Maqoud F, Antonacci M, et al. Bisphosphonates targeting ion channels and musculoskeletal effects. Front Pharmacol 2022; 13: 837534. doi: 10.3389/fphar.2022.837534.
21. Florencio-Silva R, Sasso GR, Sasso-Cerri E, et al. Biology of bone tissue: structure, function, and factors that influence bone cells. BioMed Res Int 2015; 2015: 421746. doi: 10.1155/2015/421746.
22. Hughes R, Chen X, Hunter KD, et al. Bone marrow

osteoprogenitors are depleted whereas osteoblasts are expanded independent of the osteogenic vasculature in response to zoledronic acid. FASEB J 2019; 33(11): 12768-12779.
23. Zhao C, Liu W, Zhu M, et al. Bioceramic-based scaffolds with antibacterial function for bone tissue engineering: a review. Bioact Mater 2022; 18: 383-398.
24. Cruz J, Ortiz C, Guzmán F, et al. Antimicrobial peptides: promising compounds against pathogenic micro-organisms. Curr Med Chem 2014; 21(20): 2299-2321.
25. Moghaddam MM, Barjini KA, Ramandi MF, et al. Investigation of the antibacterial activity of a short cationic peptide against multidrug-resistant *Klebsiella pneumoniae* and *Salmonella typhimurium* strains and its cytotoxicity on eukaryotic cells. World J Microbiol Biotechnol 2014; 30(5):1533-1540.
26. Hosseini Aghozbeni EA, Imani Fooladi AA, Forotan Koudehi M, et al. Use of nano-bioglass scaffold enhanced with mesenchymal stem cells for rat calvarial bone tissue regeneration. Trends Biomater Artif Organs 2014; 28(1): 8-18.
27. Amani J, Barjini KA, Moghaddam MM, et al. *In vitro* synergistic effect of the CM11 antimicrobial peptide in combination with common antibiotics against clinical isolates of six species of multidrug-resistant pathogenic bacteria. Protein Pept Lett 2015; 22(10): 940-951.
28. Abdulahy SB, Esmaeili Bidhendi M, Vaezi MR, et al. Osteogenesis improvement of gelatin-based nanocomposite scaffold by loading zoledronic acid. Front Bioeng Biotechnol 2022; 10: 890583. doi: 10.3389/fbioe.2022.890583.
29. Chizari M, Khosravimelal S, Tebyaniyan H, et al. Fabrication of an antimicrobial peptide-loaded silk fibroin/gelatin bilayer sponge to apply as a wound dressing; an *in vitro* study. Int J Pept Res Ther 2022; 28: 18. doi: 10.1007/s10989-021-10333-6.
30. Askari M, Jadid Tavaf M, Ghorbani M, et al. Electrospun propolis-coated PLGA scaffold enhances the osteoinduction of mesenchymal stem cells. Curr Stem Cell Res Ther 2024; 19(1): 94-102.
31. Sun J, Li J, Li C, et al. Role of bone morphogenetic protein-2 in osteogenic differentiation of mesenchymal stem cells. Mol Med Rep 2015; 12(3): 4230-4237.
32. Mirzaei A, Saburi E, Enderami SE, et al. Synergistic effects of polyaniline and pulsed electromagnetic field to stem cells osteogenic differentiation on poly-vinylidene fluoride scaffold. Artif Cells Nanomed Biotechnol 2019; 47(1): 3058-3066.
33. Lee JS, Choi YS, Cho SW. Decellularized tissue matrix for stem cell and tissue engineering. Adv Exp Med Biol 2018; 1064: 161-180.
34. Rubessa M, Polkoff K, Bionaz M, et al. Use of pig as a model for mesenchymal stem cell therapies for bone regeneration. Anim Biotechnol 2017; 28(4): 275-287.
35. Chen P, Liu L, Pan J, et al. Biomimetic composite scaffold of hydroxyapatite/gelatin-chitosan core-shell nanofibers for bone tissue engineering. Mater Sci Eng C Mater Biol Appl 2019; 97: 325-335.
36. Carvalho MS, Silva JC, Udangawa RN, et al. Co-culture cell-derived extracellular matrix loaded electrospun microfibrous scaffolds for bone tissue engineering. Mater Sci Eng C Mater Biol Appl 2019; 99: 479-490.
37. Ye Q, Zhang Y, Dai K, et al. Three dimensional printed bioglass/gelatin/alginate composite scaffolds with promoted mechanical strength, biomineralization, cell responses and osteogenesis. J Mater Sci Mater Med 2020; 31(9): 77. doi: 10.1007/s10856-020-06413-6.
38. Li X, Zuo S, Wang B, et al. Antimicrobial mechanisms and clinical application prospects of antimicrobial peptides. Molecules 2022; 27(9): 2675. doi: 10.3390/molecules27092675.
39. Mirnejad R, Fasihi-Ramandi M, Behmard E, et al. Interaction of antibacterial CM11 peptide with the Gram-positive and Gram-negative bacterial membrane models: a molecular dynamics simulations study. Chem Pap 2023; 77(7): 3727-3735.
40. Rončević T, Vukičević D, Krce L, et al. Selection and redesign for high selectivity of membrane-active antimicrobial peptides from a dedicated sequence/function database. Biochim Biophys Acta Biomembr 2019; 1861(4): 827-834.
41. Khalili S, Mohebali M, Ebrahimzadeh E, et al. Antimicrobial activity of an antimicrobial peptide against amastigote forms of *Leishmania major*. Vet Res Forum 2018; 9(4): 323-328.
42. Wang H, Peng T, Wu H, et al. *In situ* biomimetic lyotropic liquid crystal gel for full-thickness cartilage defect regeneration. J Control Release 2021; 338: 623-632.
43. Safari B, Aghazadeh M, Aghanejad A. Osteogenic differentiation of human adipose-derived mesenchymal stem cells in a bisphosphonate-functionalized polycaprolactone/gelatin scaffold. Int J Biol Macromol 2023; 241: 124573. doi: 10.1016/j.ijbiomac.2023.124573.
44. Yeniyol S, Ricci JL. Alkaline phosphatase levels of murine pre-osteoblastic cells on anodized and annealed titanium surfaces. Eur Oral Res 2018; 52(1):12-19.
45. Bensimon-Brito A, Cardeira J, Dionísio G, et al. Revisiting *in vivo* staining with alizarin red S - a valuable approach to analyse zebrafish skeletal mineralization during development and regeneration. BMC Dev Biol 2016; 16: 2. doi: 10.1186/s12861-016-0102-4.
46. Kannan S, Ghosh J, Dhara SK. Osteogenic differentiation potential of porcine bone marrow mesenchymal stem cell subpopulations selected in different basal media. Biol Open 2020; 9(10): bio053280. doi: 10.1242/bio.053280.